

Morphometric, immunohistochemical and ultrastructural examination of age-related structural alterations in the optic nerve

 Serpil Çilingiroğlu Anlı¹,  Engin Çalgüner²,  Deniz Erdoğan³,  Dural Kadioğlu⁴,  Çiğdem Elmas³,  Rabet Gozil⁵,  Meltem Bahçelioğlu⁶

¹Department of Anatomy, Faculty of Medicine, Kırıkkale University, Kırıkkale, Türkiye

²Department of Anatomy, Faculty of Medicine, Kyrenia University, Kyrenia, Turkish Republic of Northern Cyprus

³Department of Histology and Embryology, Faculty of Medicine, Gazi University, Ankara, Türkiye

⁴Department of Fine Arts, Faculty of Art, Design, and Architecture, Bilkent University, Ankara, Türkiye

⁵Department of Anatomy, Faculty of Medicine, Yüksek İhtisas University, Ankara, Türkiye

⁶Department of Anatomy, Faculty of Medicine, Gazi University, Ankara, Türkiye

Cite this article as: Çilingiroğlu Anlı S, Çalgüner E, Erdoğan D, et al. Morphometric, immunohistochemical and ultrastructural examination of age-related structural alterations in optic nerve. *J Health Sci Med.* 2024;7(4):416-425.

Received: 19.05.2024

Accepted: 13.07.2024

Published: 30.07.2024

ABSTRACT

Aims: As individuals age, there is a known decline in visual function attributed to a reduction in the optic nerve fibers and myelin sheath degeneration. Studies present conflicting findings on whether aging affects axonal integrity in the human optic nerve. This study aims to investigate degenerative changes in the aging rat optic nerve.

Methods: The investigation involved 36 Wistar albino rats. The rats were divided into six groups: the newborn, prepubertal, pubertal, junior, adult, and elderly groups. This study investigated optic nerve axon counts, axon diameters, levels of glial fibrillary acidic protein immunoreactivity (GFAP-IR) and nerve growth factor immunoreactivity (NGF-IR), as well as findings from light microscopy (LM) and electron microscopy (EM) in these groups.

Results: This study observed age-related alterations in rat optic nerves, including increased diameter, irregular axon count fluctuations (both increases and decreases), elevated astrocyte count, and a simultaneous decline in oligodendrocyte count. Additionally, it was observed that NGF-IR was predominantly at the membrane level in newborns and moderately in the cytoplasm, whereas in older ages, it was evident at both cellular and axonal levels furthermore, it was observed that GFAP-IR increased with age. However, in LM and EM examinations, axonal loss and rarefaction, accumulation of osmiophilic substances, splitting of the myelin sheath, vacuolization, axonal retraction were observed.

Conclusion: In this study, it was found that one of the causes of age-related vision loss is the advanced degenerative changes in the optic nerve and it was concluded that the remaining small-diameter myelinated nerve fibers may partially compensate for the sense of vision. Our study reveals that age-related degenerative changes in the central nervous system resemble those in multiple sclerosis (MS), suggesting a potential contribution to MS pathogenesis.

Keywords: Optic nerve, age-related changes, nerve growth factor, glial fibrillary acidic protein, electron microscopy, multiple sclerosis

INTRODUCTION

The optic nerve, classified as a cranial nerve, is an essential component of the visual system, composed of axons originating from retinal ganglion cells and associated glial cells. It serves the crucial function of transmitting visual information from the retina to the brain.¹

The decline of visual acuity in aging is well-documented, potentially attributed to lens opacity, age-related myopia, or reduced retinal receptors or transmitter elements. This decline may involve the optic nerve fiber reduction and myelin sheath degeneration.¹⁻⁴ Age-related morphological changes in the human optic nerve include fibrous septa expansion, corpora amylacea/lipofuscin production, gliosis, and axon loss.^{5,6}

Numerous studies have investigated age-related morphological, morphometric, immunohistochemical, or ultrastructural changes in the human and animal optic nerve.⁸⁻¹¹ The results of these studies are examined, no definite consensus has been reached regarding the outcomes. Furthermore, while some recent studies suggest a loss of axons in the human optic nerve with age, certain studies have failed to establish this relationship. Additionally, in recent years, various studies have suggested axonal loss with age in the human optic nerve, while some studies have failed to establish this relationship.^{4,7,12-14} Consequently, the functional significance of age-related changes and their impacts on impairments in visual function have not yet been fully elucidated.

Corresponding Author: Serpil Çilingiroğlu Anlı, serpilblue@gmail.com



This work is licensed under a Creative Commons Attribution 4.0 International License.

The aim of this experimental study was to identify the degenerative changes occurring in the aging optic nerve with advancing age in rats. Age-related degenerative changes in the central nervous system (CNS) including the optic nerve, exhibit significant similarities with multiple sclerosis (MS), and these changes are thought to potentially play a role in MS pathogenesis.¹⁵ Understanding these parallels could provide insights into the broader implications of the optic nerve aging and its potential relevance to neurodegenerative conditions like MS.

METHODS

This study was conducted after obtaining approval from the Gazi University of Ethics Committee for Experimental Animals (Date: 29.11.2004, Decision No: 04.030). All animal experiments were performed in accordance with the Helsinki Declaration for the use of laboratory animals. Furthermore, the use of animals in ophthalmic research adhered to the ARVO Statement for the use of animals in ophthalmic and vision research. According to this statement, a sufficient number of animals per group must be used to achieve statistical significance in animal experiments. In numerous studies similar to ours, at least 6 to 10 animals per group have been used.^{8,10,12,13,16} The rats were obtained from the Gazi University Laboratory Animal Breeding and Experimental Research Center (GUDAM). In this study, a total of 36 Wistar Albino rats spanning from birth to advanced age were divided into groups without gender discrimination as follows: newborn group (4-day-old rats, n=6), Prepuberty group (5-week-old rats, n=6), Puberty group (7-week-old rats, n=6), Junior group (early adult phase, 3-month-old rats, n=6), Adult group (1-year-old rats, n=6), Elderly group (2-year-old rats, n=6).¹⁷

Surgical Procedure

Rats were anesthetized by intraperitoneal injection of ketamine (44 mg/kg) and xylazine (5 mg/kg) followed by cardiac perfusion for euthanasia. Subsequently, euthanasia was performed, starting from the foramen magnum, a cut was made over the protuberentia occipitalis externa (inion) and extended slightly above the sagittal suture. Then, advancement was made a short distance toward the coronal sutures on both sides. Ultimately, upon opening the calvaria and lifting the frontal lobe backward, the optic chiasm was reached, and the optic nerves were extracted bilaterally to the maximum possible length. Subsequently, these extracted tissues were divided for fixation in 10% formaldehyde for light microscopy and in 2% glutaraldehyde for electron microscopy.

The methods involved in this study included histopathological examination, immunohistochemical analysis, and electron microscopy. Tissue samples were fixed in 10% buffered formaldehyde, embedded in paraffin, and sectioned at 5 μ m thickness for histopathology. Hematoxylin and eosin (H&E) and toluidine blue stains were applied, followed by axon counting in five randomly selected fields per slide. Immunohistochemistry utilized 4 μ m sections deparaffinized

in xylene, followed by antigen retrieval and incubation with primary antibodies for nerve growth factor (NGF, Santa Cruz, H-20 sc-548) and glial fibrillary acidic protein (GFAP, Ab-1 (clone GA-5), Lab Vision, MS-280-R-7). The H-SCORE method was employed for immunohistochemical evaluations.¹⁸ Electron microscopy involved fixation in glutaraldehyde, osmium tetroxide staining, and sectioning into 0.5 μ m thickness for evaluation using a transmission electron microscope (Carl Zeiss EM 900).

Statistical Analysis

The data were analyzed using the SPSS software (Statistical Package For Social Sciences, v.10.0). For comparison of non-parametric data, the Kruskal-Wallis test was employed ($p < 0.05$). Pairwise group comparisons were conducted using the Mann Whitney U test and Bonferroni correction ($p < 0.0033$). Statistical relationships between study parameters and age groups were examined using the Spearman's rho correlation test ($p < 0.05$).

RESULTS

Histopathological Examination

In sections of the optic nerve from the newborn group, it was observed that the surrounding connective tissue sheath was considerably thick, and within the inner portions, cells and myelinated nerve fibers were dispersed. Additionally, it was observed that there was a lack of gradual separation into sections of the connective tissue, and the myelin sheath was quite thin, with astrocytes and oligodendrocytes of various sizes found among fibers of different sizes. Electron microscopy sections revealed a small number of myelinated nerve fibers with small diameters, indicating highly active oligodendrocyte cytoplasm that was still in the process of forming the myelin sheath. Numerous free ribosomes and expanded granular endoplasmic reticulum (GER) tubules were observed. Mitochondria were present in low numbers and small in size. The presence of collagen fibers, which had not yet formed extensive bundles, was observed in the connective tissue. Observations indicated parallel alignment of myelin lamellae. Transverse sections of neurofilaments and neurotubules were observed in the axon (Table 1, Figure 1).

In tissue samples from the prepubertal group, the optic nerve appeared more organized, with a distinct connective tissue capsule, the emergence of myelin sheaths, and the presence of mature astrocytes alongside oligodendrocytes located closer to myelinated axons. At the end of the immunohistochemical staining, it was observed that NGF immunoreactivity (IR) was predominantly around the fibers and varied in intensity from moderate to strong intermittently. It was noteworthy that astrocyte feet were also stained on the vessel wall. In this group, it was observed that GFAP-IR was prominent in fully differentiated astrocytes. The structure of the axon was well-preserved. It was observed that small fibers were in normal structure, whereas larger fibers exhibited separations between myelin lamellae (Table 1, Figure 2).

Table 1. Findings of Toluidine blue stains, GFAP, NGF, and the electron microscopy by different age groups in rats

Groups	Toluidine blue stains	GFAP	NGF	The electron microscopy
Newborn	The peripheral connective tissue sheath of the OP was quite thick. The myelin sheath was noted to be quite thin, and OL of various sizes were present among the small and large fibers	The GFAP-IR revealed a reaction that was not entirely specific, indicating cells differentiating into AST and occasional involvement observed in the membrane and cytoplasm	The NGF-IR was predominantly observed at the membrane level, with moderate cytoplasmic involvement	Within the cytoplasm of the OL forming the myelin sheath, tubules of expanded the GER, RI, and M were observed. Additionally, along with KO that did not form bundles in the connective tissue. Sections of NF and NT in A, arranged in parallel with each other along with myelin lamellae, were observed
Prepubertal	The OP appeared more organized and the connective tissue capsule was pronounced. The presence of myelin sheath development was evident, along with mature AST, and the distinguishable proximity of OL to myelinated axons was identified	Distinct GFAP-IR was detected in AST	The NGF-IR was predominantly observed at the periphery of the fibers	Large-diameter A exhibiting separation between lamellae were observed alongside small-diameter myelinated axons
Puberty	The connective tissue sheath of the OP resembled a mature structure. The myelin sheath showed a mature-like structure, and the presence of AST and OL among them was distinguished	Highly intense immunoreactivity of GFAP was detected in the cytoplasm of AST	Distinct NGF-IR was observed both in glial cells and their extensions	Occasional separations were observed in myelinated nerve fibers, OL, C, A, NF, and NT
Junior	The connective tissue surrounding the OP was observed. Extensive connective tissue partitions, AST, and OL were identified. Axons with normal structure alongside axons showing degeneration in the myelin sheath were detected	Significantly specific and intense GFAP-IR was detected in the cytoplasm of Ast and their extensions	It was observed in tissue samples that the NGF-IR was very weak throughout the tissue	Occasional expanded GER tubules were observed in the OL and cell cytoplasm. Small-diameter myelinated fibers were observed in their normal structure, disruptions were seen in large-diameter myelin fibers, and the A were observed to retract
Early adult	The connective tissue surrounding the OP was observed. Expanses of connective tissue sections, AST and OL were identified. Myelinated axons in their normal structure, and axons displaying degeneration in the myelin sheath were detected	The GFAP-IR was detected in AST	The NGF-IR was observed at axonal and cellular levels	Along with small-diameter fibers observed in normal structure, splittings and loss in the myelin of larger fibers, VA, OS, axonal retraction were observed. The splitting caused by separation in some myelin sheaths was observed
Elderly	The OP was enclosed by connective tissue. Extensive partitions of connective tissue were observed, along with AST and OL. Myelinated axons in their normal structure, as well as axons showing degeneration within the myelin sheath, were detected	Distinctive GFAP-IR was observed in AST	The NGF-IR was observed at both axonal and cellular levels	The OL were observed in their normal structure, along with C and small-diameter myelinated nerve fibers. Lamellar losses in the myelin sheath were observed in large-diameter fibers, along with splitting and axonal retraction. Crystallization was observed in axonal M

The optic nerve (OP), oligodendrocytes (OL), astrocytes (Ast), glial fibrillary acidic protein immunoreactivity (GFAP-IR), nerve growth factor immunoreactivity (NGF-IR), granular endoplasmic reticulum (GER), ribosomes (Ri), mitochondria (M), collagen fibers (Ko), neurofilaments (Nf), neurotubules (Nt), axon (A), cell nucleus (C), vacuolization (Va), osmiophilic substance accumulation (Os), cell nuclei (C)
GFAP: Glial fibrillary acidic protein, NGF: Nerve growth factor, IR: Immunoreactivity

In the optic nerve sections from the puberty group, the nerve appeared considerably developed, with the connective tissue sheath and myelin sheath showing correspondingly mature structures, and the presence of astrocytes and oligodendrocytes among them was observed. Furthermore, it was observed that there was a varying degree of NGF-IR, ranging from moderate to strong, both in glial cells and at the membrane level, while a highly intense GFAP-IR was detected in the astrocyte cytoplasm. Electron microscope examinations revealed the mature structures of oligodendrocytes. The nucleus and cytoplasm did not show any signs of degeneration. The myelinated nerve fibers appeared considerably developed, although some of them exhibited occasional separations. Axons displayed a normal structure. Neurofilaments and neurotubules were prominently visible (Table 1, Figure 3).

In the junior group, it was observed that the optic nerve reached normal diameter, and both cellular and fiber distribution along with the connective tissue sheath became more pronounced. Additionally, it was observed that the optic nerve appeared to be divided into lobes due to extensive connective tissue partitions. There was a noticeable increase in the number of astrocytes, while oligodendrocytes appeared to be in their normal structure. There was observed

significant degeneration in some large-diameter myelinated axons, which were filled with connective tissue in those areas. In this group, it was determined that the NGF-IR was very weak throughout the tissue. In the same group, GFAP-IR was observed to be quite intense in the astrocyte cytoplasm and its extensions. Under the electron microscope, it was observed that oligodendrocytes exhibited mature structures, characterized by heterochromatic nuclei and dense cytoplasm. Occasionally, expanded GER tubules were prominent in the cell cytoplasm. While small-diameter myelin fibers appeared normal, intermittent separations were observed in large-diameter myelin fibers, along with axonal retraction and increased interstitial connective tissue between fibers (Table 1, Figure 4).

In adult rats, it was observed that structural changes during the early adult period continued to increase. It was determined that there was NGF-IR at both axonal and cellular levels in the immunohistochemical sections. While GFAP-IR was observed at the level of astrocyte extensions, it was noted that in areas where fiber degeneration was highly noticeable, the immunoreactivity was not specific. It appeared intermittently weak in the astrocyte cytoplasm and occasionally present in the membrane. The electron microscope examination revealed that small-diameter fibers were normal. However, in the

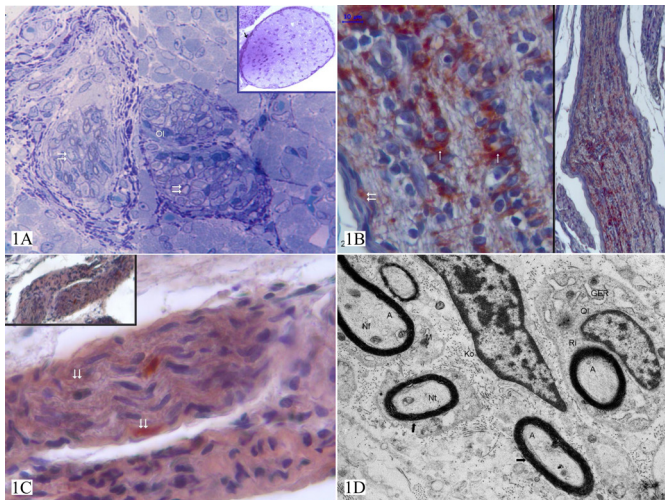


Figure 1. In tissue samples from the newborn group (1A), it was observed that the peripheral connective tissue sheath of the optic nerve was quite thick (f). The myelin sheath (z) was noted to be quite thin, and oligodendrocytes (Ol) of various sizes were present among the small and large fibers (Toluidine blue, x40, x1000). (1B) The immunohistochemical staining of GFAP revealed a reaction that was not entirely specific, indicating cells differentiating into astrocytes (f) and occasional involvement observed in the membrane and cytoplasm (z) (Immunoperoxidase & Hematoxylin, x100, x400). Observations in (1C) showed that NGF-IR was predominantly at the membrane level (ll), with moderate cytoplasmic involvement and (immunoperoxidase & hematoxylin, x100, x400). (1D) In the electron microscopy, within the cytoplasm of oligodendrocytes (Ol) forming the myelin sheath, tubules of expanded granular endoplasmic reticulum (GER), free ribosomes (Ri), and mitochondria (M) were observed, along with collagen fibers (Ko) that did not form bundles in the connective tissue. Sections of neurofilaments (Nf) and neurotubules (Nt) in the axon (A), arranged in parallel with each other along with myelin lamellae (h), were observed. (uranium acetate-lead citrate, x7000)

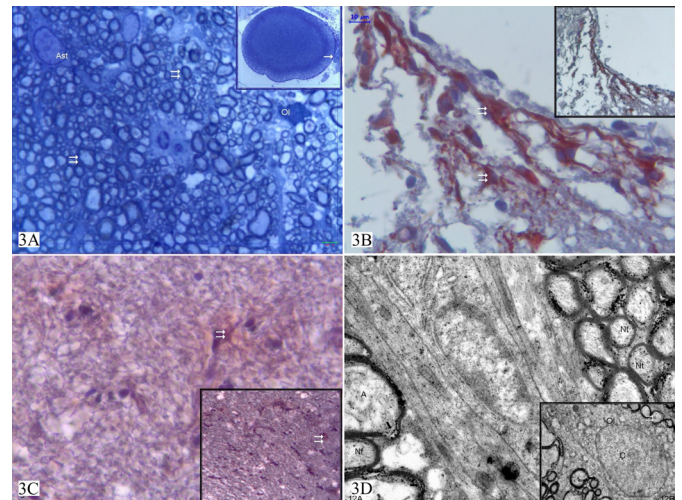


Figure 3. Regarding tissue samples from the puberty group (3A), it was observed that the connective tissue sheath (h) of the optic nerve resembled a mature structure. The myelin sheath (z) showed a mature-like structure, and the presence of astrocytes (Ast) and oligodendrocytes (Ol) among them was distinguished (Toluidine blue, x40, x1000). (3B) In the immunohistochemical staining performed with GFAP, a highly intense immunoreactivity was detected in the cytoplasm of astrocytes (z) (immunoperoxidase & hematoxylin, x100, x400). (3C) Additionally, distinct NGF-IR was discerned both in glial cells and their extensions (z) (immunoperoxidase & hematoxylin, x100, x400). (3D) In the electron microscopic image, oligodendrocytes (Ol), cell nucleus (C), occasional separations in myelinated nerve fibers (h), axon (A), neurofilaments (Nf), and neurotubules (Nt) were observed (uranium acetate-lead citrate, x 3000, x 12000)

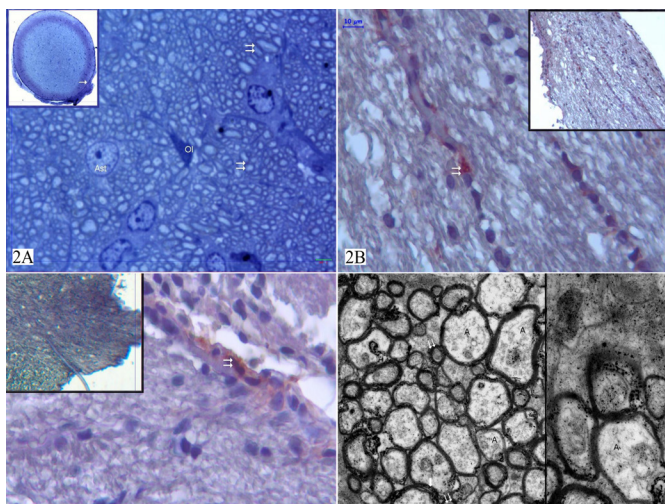


Figure 2. Regarding tissue samples from the prepubertal group (2A), it was observed that the optic nerve appeared more organized and the connective tissue capsule (h) was pronounced. The presence of myelin sheath (z) development was evident, along with mature astrocytes (Ast), and the distinguishable proximity of oligodendrocytes (Ol) to myelinated axons was identified (Toluidine Blue, x40, x1000). (2B) Distinct GFAP-IR was detected in astrocytes (z) (Immunoperoxidase & Hematoxylin x100, x400). (2C) The NGF-IR was predominantly observed at the periphery of the fibers (z) (Immunoperoxidase & Hematoxylin, x100, x400). (2D) In the electron microscope image, large-diameter axons (A) exhibiting separation between lamellae (h) were observed alongside small-diameter myelinated axons (ll) (uranium acetate-lead citrate, x 4400, x 7000)

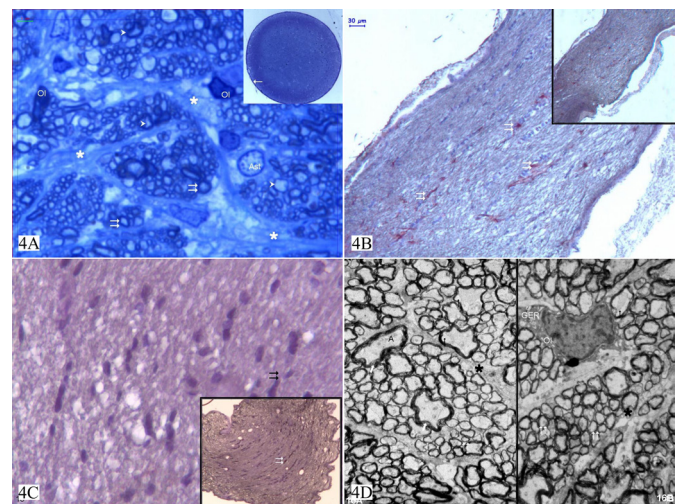


Figure 4. In tissue samples from the Junior group (4A), connective tissue (h) surrounding the optic nerve was observed. Additionally, extensive connective tissue (*) partitions, astrocytes (Ast), and oligodendrocytes (Ol) were identified. Axons with normal structure (z) alongside axons showing degeneration in the myelin sheath (h) were detected (Toluidine blue, x40, x1000). In (4B), significantly specific and intense GFAP-IR was detected in the cytoplasm of astrocytes (z) and their extensions (immunoperoxidase & hematoxylin, x100, x400). In tissue samples (4C), it was observed that the NGF-IR was very weak throughout the tissue (z) (Immunoperoxidase & Hematoxylin, x100, x400). In electron microscope images (4D), occasional expanded GER tubules were observed in the oligodendrocyte (Ol) and cell cytoplasm. Small-diameter myelinated fibers were observed in their normal structure (ll), disruptions were seen in large-diameter myelin fibers (h), and the axon (A) was seen to retract (*) (uranium acetate-lead citrate, x3000)

myelin of large-diameter fibers, separations, vacuolization, and accumulation of osmiophilic material were observed, and axonal retraction and splitting were detected in some myelin sheaths (Table 1, Figure 5).

In the optic nerve sections of the elderly group, there was remarkable degeneration in the myelin of thick axons and loss of myelin in thin axons. The connective tissue divisions between the axons were extremely thickened, and loss of astrocytes

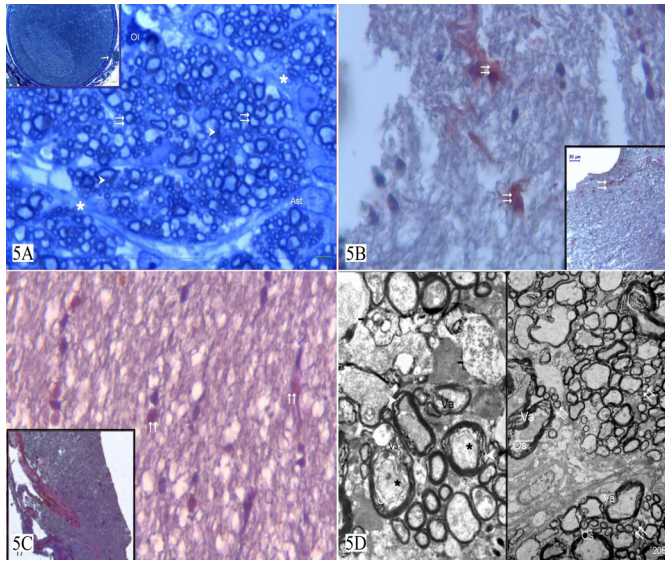


Figure 5. In tissue samples from the adult group (5A), the connective tissue surrounding the optic nerve was observed (↔). Furthermore, expanses of connective tissue sections (*), astrocytes (Ast), and oligodendrocytes (Ol) were identified. Myelinated axons in their normal structure (→), and axons displaying degeneration in the myelin sheath (▶) were detected (Toluidine blue, x40, x1000). (5B) GFAP-IR (→) was detected in astrocytes (Immunoperoxidase & Hematoxylin, x100, x400). (5C) Additionally, NGF-IR (▶) was observed at axonal and cellular levels (immunoperoxidase & hematoxylin, x100, x400). (5D) In electron microscope images, along with small-diameter fibers observed in normal structure (▶), splittings and loss in the myelin of larger fibers (▶), vacuolization (Va), osmiophilic substance accumulation (Os), axonal retraction (*) were observed. The splitting caused by separation in some myelin sheaths (▶) was observed (uranium acetate-lead citrate, x3000)

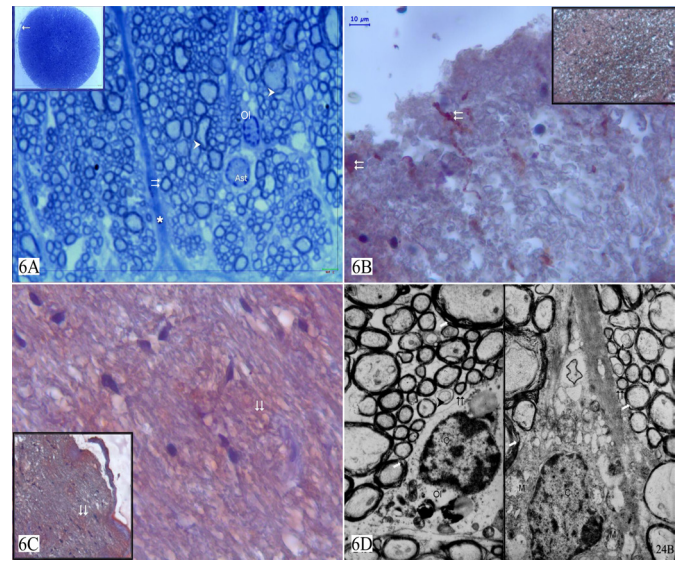


Figure 6. The optic nerve was enclosed by connective tissue (↔), as observed in tissue samples from the elderly group (6A). Moreover, extensive connective tissue (*) partitions were observed, along with astrocytes (Ast) and oligodendrocytes (Ol). In addition to normal structured myelinated axons (→), axons showing degeneration within the myelin sheath (▶) were detected (Toluidine blue, x40, x1000). (6B) Observed GFAP-IR distinctively present in astrocytes (→) (immunoperoxidase & hematoxylin, x100, x400). (6C) Besides, NGF-IR was seen at the axonal and cellular levels (▶) (immunoperoxidase & hematoxylin, x100, x400). (6D) In the electron microscopic images, oligodendrocytes (Ol) observed in normal structure, along with cell nuclei (C) and small-diameter myelinated nerve fibers (▶). Lamellar losses in the myelin sheath were observed in large-diameter fibers (▶) (white arrow), along with splitting (▶) and axonal retraction (▶). Crystallization was observed in axonal mitochondria (M) (uranium acetate-lead citrate, x3000)

was also observed in some places. The oligodendrocytes were in sight in small numbers. Immunohistochemical sections from this group demonstrated the presence of NGF-IR at both axonal and cellular levels, similar to the adult group. Within this group, GFAP-IR was observed at the level of the foot processes of astrocyte. It was noted that in areas with marked fiber degeneration, the immunoreactivity was not specific, displaying a weakened intensity in astrocytic cytoplasm and occasionally involving the membrane. In the electron microscopic examination, various forms of myelin degeneration were commonly detected. While small diameter fibers were perceived normally, in large diameter fibers, splitting along with occasional lamellar losses in the myelin sheath and axonal retraction captured notice. Additionally, crystalalysis was observed in mitochondria (Table 1, Figure 6).

Morphometric Analysis

The measurements of the optic nerve’s diameter (X²=27.853, p<0.001), axon counts (X²=19.385, p<0.001), GFAP-IR (X²=32.558, p<0.001), and NGF-IR (X²=26.661, p<0.001) immunoreactivity levels were found to differ among the groups (Table 2). However, following pairwise group comparisons, no statistical difference was found between the groups (p>0.0033) (Table 3, Figure 7).

The correlation analysis revealed a positive correlation between age group and axon diameter (r=0.770, p<0.001) as well as between axon diameter and NGF-IR H-score (r=0.482, p=0.003). Based on these results, it was considered that in rats, axon diameter values may increase with aging, and as axon diameter increases, NGF-IR may also increase. As a result, it was argued that NGF-IR may increase indirectly with aging.

Table 2. A descriptive table illustrating the optic nerve axon count results, axon diameter measurements, GFAP-IR H-score values, and NGF-IR H-score values of the study groups

Variable	Groups	Median (min-max)	x ²	p
Axon count	Newborn	149.50 (126-172)	19.385	0.002
	Pre-puberty	188 (144-218)		
	Puberty	121 (83-155)		
	Junior	166 (146-188)		
	Adult	136.50 (53-156)		
	Elderly	158 (123-169)		
Axon diameter	Newborn	258.38 (224.18-296.18)	27.853	<0.001
	Pre-puberty	494.11 (481.55-516.09)		
	Puberty	555.16 (489.63-608.16)		
	Junior	499.29 (494.80-510.62)		
	Adult	618.02 (572.13-623.21)		
	Elderly	579.86 (561.83-597.51)		
GFAP	Newborn	62 (57-69)	32.558	<0.001
	Pre-puberty	57.50 (56-62)		
	Puberty	80 (75-84)		
	Junior	76.50 (70-84)		
	Adult	40 (36-47)		
	Elderly	29 (23-32)		
NGF	Newborn	45.50 (44-50)	26.661	<0.001
	Pre-puberty	69 (60-75)		
	Puberty	64.50 (59-68)		
	Junior	28 (27-31)		
	Adult	64.50 (60-69)		
	Elderly	63.50 (57-70)		

GFAP: Glial fibrillary acidic protein, NGF: Nerve growth factor, IR: Immunoreactivity, Kruskal-Wallis test, p<0.05

Table 3. The binary group comparison results of the optic nerve axon count outcomes, axon diameter measurements, GFAP-IR H-score values, and NGF-IR H-score values for the study groups

Groups (I/J)	Axon count		Axon diameter		GFAP		NGF	
	z	p	z	p	z	p	z	p
Newborn/pre-puberty	-2.326	0.020	-2.882	0.004	-1.621	0.105	-2.887	0.004
Newborn/puberty	-2.005	0.045	-2.882	0.004	-2.892	0.004	-2.887	0.004
Newborn/junior	-1.761	0.078	-2.882	0.004	-2.892	0.004	-2.908	0.004
Newborn/adult	-1.121	0.262	-2.882	0.004	-2.898	0.004	-2.892	0.004
Newborn/elderly	-0.321	0.748	-2.882	0.004	-2.892	0.004	2.982	0.004
Pre-puberty/puberty	-2.722	0.006	-1.441	0.150	-2.892	0.004	-1.690	0.091
Pre-puberty/junior	-1.601	0.109	-0.641	0.522	-2.892	0.004	-2.903	0.004
Pre-puberty/adult	-2.402	0.016	-2.882	0.004	-2.898	0.004	-1.457	0.145
Pre-puberty/elderly	-2.085	0.037	-2.882	0.004	-2.892	0.004	-1.848	0.065
Puberty/junior	-2.722	0.006	-1.441	0.150	-0.964	0.335	-2.903	0.004
Puberty/adult	-0.320	0.749	-2.242	0.025	-2.887	0.004	-0.405	0.685
Puberty/elderly	-2.246	0.025	-0.961	0.337	-2.882	0.004	-0.727	0.467
Junior/adult	-2.486	0.013	-2.882	0.004	-2.887	0.004	-2.908	0.004
Junior/elderly	-1.451	0.147	-2.882	0.004	-2.882	0.004	-2.908	0.004
Adult/elderly	-1.925	0.054	-1.922	0.055	-2.887	0.004	-0.808	0.419

GFAP: Glial fibrillary acidic protein, NGF: Nerve growth factor, IR: Immunoreactivity, Mann-Whitney u test and Bonferroni correction test, p<0.0033

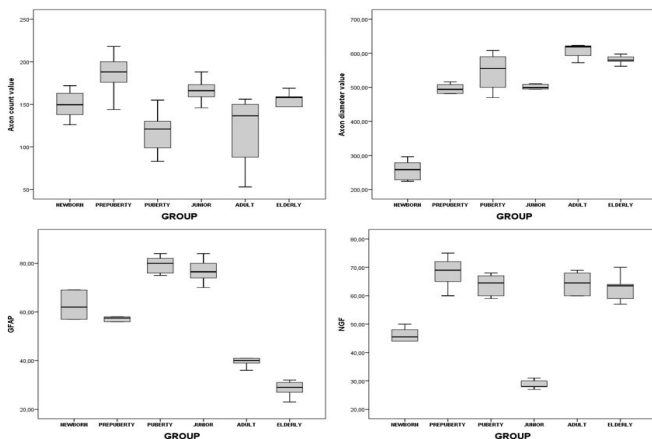


Figure 7. There are no statistically significant differences in the pairwise group comparisons of axon count value, axon diameter value, GFAP-IR, and NGF-IR for each age group

Additionally, a negative correlation was found between age group and GFAP-IR ($r=-0.504$, $p=0.002$) as well as between axon diameter value and GFAP-IR ($r=-0.402$, $p=0.015$) (Table 4). As a result, it was considered that GFAP-IR may decrease with aging in rats, and it was further thought that GFAP-IR values may decrease if axon diameter increases.

DISCUSSION

Associated with aging, as in many other organs in the living organism, the eye also presents numerous irreversible and severe lesions. Decreased visual acuity, visual field, contrast sensitivity, motion perception, and dark adaptation are among the impairments observed in the elderly.¹⁹ The human optic nerve is estimated to have between 40,000 and 1,435,453 nerve fibers. Nevertheless, despite a decrease observed in the human optic nerve axons concerning age in conducted

Table 4. The statistical correlation among the study data can be observed

Groups	r	Axon count	Axon diameter	GFAP	NGF
Axon count	1.000	1.000	-0.138	0.770	-0.504
Axon diameter			1.000	-0.402	0.482
GFAP				1.000	-0.309
NGF					1.000

GFAP: Glial fibrillary acidic protein, NGF: Nerve growth factor

studies, it has been reported that this decline lacks statistical significance.⁷ On the other hand, it has been reported that the axon numbers in the human embryonic optic nerves taken between weeks 8-18 of pregnancy reach their peak during the 3rd and 4th months and subsequently decline.²⁰ Although the developing adult rodents' visual system has been extensively investigated using morphological, physiological, biochemical, and behavioral techniques, age-related alterations in the rat's optic nerve have not been evaluated by combining various methods including morphological, immunohistochemical, and ultrastructural analyses. Therefore, there has been no consensus among the results.^{8,10,19,21}

In the conducted studies, it has been reported that while the number of optic nerve fibers remains unchanged in adult rats, it gradually decreases in elderly rats.^{16,22,23} Meanwhile, Lam et al.²⁴ compared the number of axons in the optic nerve

of newborn and adult rats, concluding that approximately 60% of the axons present in the optic nerve at birth were lost during the adult stage.

Our study revealed a significant statistical difference in both the number and diameter of the optic nerve across different age groups. However, after conducting pairwise group comparisons, no substantial differences were detected among the groups. The results indicated that the numbers and diameters of axons within the optic nerve remained unchanged with age. However, when numerical data is considered, it is observed that the number of axons showed a significant increase in the prepubertal age group, but this count decreased to a similar level as other age groups with the puberty. Moreover, it has been observed that while the axon numbers are low in newborns, they elevate during the prepuberty stage, decrease to the levels of the neonatal period during puberty, subsequently rise again during junior period before declining once more in the adult stage, and exhibit an increase again in the elderly group. Based on this, it was hypothesized that there is a circadian pattern of increase and decrease in axon numbers.

Godlewski¹⁰ examined the morphology of the optic nerve myelin fibers in aging rats and reported that with aging, both the number of myelin lamellae and the interlamellar distance increased. Consequently, an increase in myelin sheath thickness was observed; however, in the oldest rats (2.5 years), this thickness had decreased again. Furthermore, Wong et al.²⁵ identified in their study on the optic nerve of young and old mice that the progression of age was concurrent with an increasing degeneration in large-diameter myelinated fibers.

According to our study, it was observed that degeneration in large-diameter myelinated fibers commences with the progression of age and continues to increase gradually. In the adult and elderly groups, age-related degenerative changes such as the division of the myelin sheath, lamellar loss and retraction, were observed. Additionally, although pairwise comparisons did not reveal statistically significant differences in the diameter values of axons located within the optic nerve among the groups, upon examining the numerical values, it was observed that axon diameters in rats during the newborn period were initially thin, but gradually increased with age. The diameter values peaked in the adult group, and a slight reduction was noted in the elderly group. Considering this, it was hypothesized that axon diameter values also exhibited a circadian rhythm in parallel with axon numbers. These findings were thought to be associated with age-related changes in hormonal processes among the subjects. However, as serum hormone levels were not included in this study, this hypothesis remained untestable.

Two distinct astrocyte shapes have been distinguished in the human optic nerve head. Thin-bodied astrocytes are positioned on blood vessels in a perforated structure through which axons pass. Thick-bodied astrocytes, on the other hand, create glial tubes directing axons towards the lamellar region.²⁶ The section of the human optic nerve head in double-antibody immunofluorescent studies has revealed a distinct presence of type IV collagen and laminin within

the extracellular matrix of the lamina cribrosa sclerae. These macromolecules are arranged transversely along nerve fascicles, forming lamellated and cribriform plates. While relatively low levels of type III and type I collagen were found in the extracellular matrix of these tissues, fibronectin was not detected.²⁷ On the other hand, Hernandez et al.²⁸ utilized immunofluorescence staining to investigate age-related changes in the human optic nerve head. They found age-related alterations in the density of type I and III collagen, as well as elastin, which contribute to the connective tissue support of nerve bundles due to the expansion of pores in the cribriform plates with age. Additionally, they observed that type IV collagen covered the cribriform planes similar to the basal membrane. If the increased collagen and elastin are considered to be responsible for the increased connective tissue area associated with aging, and if there is a gradual loss in axons of the optic nerve with age, the data obtained from our study suggests that the extracellular matrix material, which contains the fibrillar forms of collagen and elastin, fills the space of the lost tissue.

Butt and Kirvell²¹ conducted a study by immunohistochemically labeling the glial cells in the optic nerve of immature and mature rats, and observed a significant axonal loss in the optic nerves after 21 days (mature). They observed a homogeneous glial scar tissue formed by dense astrocytic extensions along the degenerating axon fibers in the nerve. In this glial scar tissue, oligodendrocytes persisted independently of the axon, and it was stated that inefficient myelin phagocytosis possibly resulted from incomplete activation of microglial macrophages. In our study, it was observed that in the adult and elderly groups, lost optic nerve fibers were replaced by glial cells and their foot processes. Consequently, it was thought that glial scar tissue was formed in this way. Cavallotti et al.⁸ investigated age-related changes in the optic nerve using the GFAP-IR staining method in 3-month-old (young), 1-year-old (adult), and 2-year-old (elderly) male rats. They demonstrated the presence of the blood-brain barrier between astrocytes, the capillary network, and axons, indicating the probable assumption of the role of myelin by glial cells (including astrocytes). However, they found no change in the protein quantity with the increase in age. Additionally, an increase in the meningeal sheath of the optic nerve, an augmentation in the number of astrocytes, enhanced regional density of GFAP-IR, enlargement in the diameter and area of the optic nerve, coupled with a decrease in the number of nerve fibers, a reduction in the dimensions of nerve fibers, and a decrease in the nerve fibers/meningeal sheath ratio from 3/1 to 1/1 were observed. In the study conducted by Cepurna et al.,²⁹ it was observed that the decrease in the number of axons significantly increased with age, however, they have determined that there was no significant change in the last months of the lives of elderly rats in terms of the decrease in the number of axons and the rate of axonal degeneration. This study does not support the linear decline in the number of optic nerve axons with age in adult rats, as demonstrated by some studies.

Our study utilized the GFAP primary antibody to identify astrocytes in experimental groups composed of different

age ranges, revealing GFAP-IR starting from the fourth day after birth. As age advanced, there was a higher specificity of immunoreactivity observed in both the cytoplasm of astrocytes and where astrocytic cytoplasmic extensions terminate at capillaries, as well as around the pia mater. Additionally, it was observed that degeneration in the myelin sheath increased progressively with advancing age, starting from the adult group. Especially in the adult and elderly groups, while small-diameter myelinated fibers were observed to maintain their normal structure, substantial disruption, vacuolization, osmiophilic material accumulation, and axonal retraction were notably observed in large-diameter myelinated fibers. The losses in certain myelin lamellae and the accompanying splitting have been identified. During this process, mature structures of astrocytes and oligodendrocytes were observed, characterized by heterochromatic nuclei and dark cytoplasm. In the cytoplasm of oligodendrocytes, enlarged GER tubules were distinctly localized.

On the other hand, it was observed that the immunohistochemical examination scores differed significantly among the groups. However, pairwise group comparisons did not reveal any statistically significant differences between the groups. However, when the numerical values of GFAP-IR scores were examined, it was observed that the scores were higher during the newborn period, decreased during the prepubertal phase, increased again during puberty, and exhibited a linear decrease during the junior, adult, and elderly periods. Therefore, it was observed that GFAP-IR exhibits a fluctuating rhythm in terms of axon count and diameter values as age progresses, along with the possibility of an increase in astrocyte numbers while axon count and diameter decrease.

According to the immunohistochemical examination conducted with NGF, the involvement of the NGF antibody in the optic nerve was observed at the meningeal level in neonates; however, as age progressed, it was noted to be present at both the cellular and axonal levels. Additionally, at the conclusion of light microscopy and electron microscopy evaluations, it was observed that there were remarkably few connective tissue septa among myelinated nerve fibers in the newborn (4-day-old) group. With the progression of age, degeneration was observed in the myelinated nerve fibers of the rat's optic nerve, and it was noted that these areas were filled with connective tissue. Furthermore, despite the finding that NGF-IR scores did not differ among the groups, upon numerical examination, it was observed that NGF-IR scores exhibited a rhythm paralleling the increase and decrease in axon count and diameter.

Godlewski¹⁰ investigated the myelin fibers in the optic nerve of elderly rats using an electron microscope and argued that there was thickening in the myelin sheath. He proposed that the increase in this thickness occurred not only due to the growth in the number of myelin lamellae but also because of the increase in interlamellar spaces. Additionally, it has been concluded that as age progresses, it may lead to morphometric changes in axonal myelin sheaths and cell membranes (edema, excessive accumulation of other lipids such as cholesterol, sphingomyelin, etc.).

In our study, it was found that the formation of myelin lamellae begins in neonates and becomes more pronounced in the prepubertal group, where slight openings are observed. In the puberty and junior groups, there is an increasing degeneration and connective tissue, whereas in the adult and elderly groups, distinct degenerative features (vacuolization, splitting, retraction, osmiophilic accumulation) manifest prominently.

The findings of our study have detailed the degenerative changes occurring in the optic nerve of rats during the aging process. These changes include axonal loss, myelin sheath fragmentation, an increase in the number of astrocytes, and a decrease in the number of oligodendrocytes. These results demonstrate the adverse effects of aging on the CNS.

MS is a chronic autoimmune disease characterized by the loss of myelin and consequent axonal degeneration in the CNS, including the optic nerves. MS and the aging process share similar degenerative changes within the CNS. In the literature, it has been reported that neurodegenerative changes increase with age in patients with MS, and the clinical course of the disease deteriorates.¹⁵

One significant concern in MS patients is the degeneration of the optic nerve, which can lead to visual impairment. Studies have shown that as patients with MS age, the risk of the optic nerve degeneration increases, which is often assessed using optical coherence tomography to monitor retinal nerve fiber layer thinning.³⁰ Trans-synaptic degeneration, where damage extends from the optic nerve to the brain, is another critical aspect of MS-related optic neuropathy. This degeneration can lead to further complications, including cortical thinning and broader neural damage, impacting overall neurological function.³¹ Research has highlighted that age-related changes exacerbate these degenerative processes, making early diagnosis and intervention crucial for managing MS patients.^{30,31}

In MS, particularly in its progressive forms, the breakdown of the myelin sheath, axonal loss, activation of glial cells, and neuroinflammation play significant roles.³²

In one study, similar changes were observed in the aging rat optic nerve. For example, findings included increased GFAP-IR levels with aging, myelin sheath fragmentation and axonal loss, an increase in the number of astrocytes, and a decrease in the number of oligodendrocytes. These findings indicate that the aging process aligns with the pathological mechanisms observed in MS.^{33,34}

The findings from our study detail the degenerative effects of aging on the CNS and reveal significant similarities when compared to MS. These similarities suggest that the degenerative changes observed during the aging process may contribute to MS pathogenesis. Therefore, further research is needed to better understand the relationship between aging and MS.

Limitations

This study exhibits certain limitations. Primarily, it was conducted using experimental animals. As the optic nerve of human cadavers was not examined or compared in this study,

the direct applicability of its findings to humans is constrained. However, when the results of the study are considered, the contention arose that conducting this research on human cadavers might be deemed suitable and could potentially illuminate novel avenues for further inquiry. Furthermore, upon reviewing the literature, it was observed that there have been very few studies examining the aging processes of the optic nerve in neonatal, prepubertal, and pubertal rats. Thus, it was contended that this study might exhibit a preliminary research character. Secondly, due to certain economic and technical constraints, advanced biochemical analysis methods (such as ELISA, Western Blot, etc.) were not employed in the examination of tissue materials related to this study. Consequently, the assessment of apoptosis, autophagy, collagen formation, other inflammatory cascades, hormonal interactions, and their outcomes concerning tissue-level aging could not be established.^{27,35} Thirdly, the optic nerves of subjects within the groups could not be analyzed using radiological imaging methods such as MRI. Finally, due to this study being conducted on experimental animals, age-related variations in visual function losses could not be determined.

CONCLUSION

At the conclusion of this study, an increase in the diameter of the optic nerve (n. opticus), irregular increments and decrements in axon count, an elevation in astrocyte numbers, and a corresponding decrease in oligodendrocyte count were observed in correlation with aging in rats. Moreover, it was observed that NGF-IR was predominantly at the membrane level in neonates and moderately present in the cytoplasm. However, with advancing age, it became evident at both the cellular and axonal levels. Additionally, an increase in GFAP-IR was observed with age. On the other hand, light microscopic and electron microscopic findings revealed axonal loss and attenuation, accumulation of osmiophilic material, myelin sheath splitting, vacuolization, axonal retraction, and replacement of lost fibers by connective tissue and glial scar formation. As a result, it was concluded that one of the reasons for the vision loss that occurs with advancing age is the progressive degenerative changes in the optic nerve. It was also inferred that the remaining small-diameter myelinated nerve fibers that are intact may compensate to some extent for visual sensation.

ETHICAL DECLARATIONS

Ethics Committee Approval

The study was approved the permission of Animal Studies Ethics Committee of Gazi University (Date: 29.11.2004, Decision No: 04.030).

Informed Consent

In this animal study, informed consent is not need.

Referee Evaluation Process

Externally peer-reviewed.

Conflict of Interest Statement

The authors have no conflicts of interest to declare.

Financial Disclosure

This study was funded by a Scientific Research Projects (SRP) grant from Gazi University.

Author Contributions

All of the authors declare that they have all participated in the design, execution, and analysis of the paper, and that they have approved the final version.

Acknowledgements

We would like to express our sincere gratitude to Prof. Bülent Bakar, Department of Neurosurgery, Kırıkkale University Faculty of Medicine for his invaluable guidance, insightful suggestions, and unwavering support throughout the course of this research. With gratitude, we express our appreciation to Bahar Kartal, MD, for her invaluable contributions to the immunohistochemical evaluations presented in the manuscript.

REFERENCES

1. De Moraes CG. Anatomy of the visual pathways. *J Glaucoma*. 2013;(22)5:2-7. doi: 10.1097/IJG.0b013e3182934978
2. Shao Y, Li L, Peng W, Lu W, Wang Y. Age-related changes in the healthy adult visual pathway: evidence from diffusion tensor imaging with fixel-based analysis. *Radiologie (Heidelb)*. 2023;63(2):73-81. doi: 10.1007/s00117-023-01192-x
3. Trinh M, Kalloniatis M, Alonso-Caneiro D, Nivison-Smith L. High-density optical coherence tomography analysis provides insights into early/intermediate age-related macular degeneration retinal layer changes. *Invest Ophthalmol Vis Sci*. 2022;63(5):36. doi: 10.1167/iovs.63.5.36
4. Balazsi AG, Rootman J, Drance SM, Schulzer M, Douglas GR. The effect of age on the nerve fiber population of the human optic nerve. *Am J Ophthalmol*. 1984;97(6):760-766. doi: 10.1016/0002-9394(84)90509-9
5. Vrabec F. Age changes of the human optic nerve head. A neurohistologic study. *Albrecht Von Graefes Arch Klin Exp Ophthalmol*. 1977;202(3):231-236. doi: 10.1007/BF00407873
6. Dolman CL, McCormick AQ, Drance SM. Aging of the optic nerve. *Arch Ophthalmol*. 1980;98(11):2053-2058. doi: 10.1001/archophth.1980.01020040905024
7. Repka MX, Quigley HA. The effect of age on normal human optic nerve fiber number and diameter. *Ophthalmology*. 1989;96(1):26-32. doi: 10.1016/s0161-6420(89)32928-9
8. Cavallotti C, Cavallotti D, Pescosolido N, Pacella E. Age-related changes in rat optic nerve: morphological studies. *Anat Histol Embryol*. 2003;32(1):12-16. doi: 10.1046/j.1439-0264.2003.00431.x
9. El-Sayyad HI, Khalifa SA, El-Sayyad FI, Al-Gebaly AS, El-Mansy AA, Mohammed EA. Aging-related changes of optic nerve of Wistar albino rats. *Age (Dordr)*. 2014;36(2):519-532. doi: 10.1007/s11357-013-9580-5
10. Godlewski A. Morphometry of myelin fibers in corpus callosum and optic nerve of aging rats. *J Hirnforsch*. 1991;32(1):39-46.
11. Sandell JH, Peters A. Effects of age on the glial cells in the rhesus monkey optic nerve. *J Comp Neurol*. 2002;445(1):13-28. doi: 10.1002/cne.10162

12. Cavallotti C, Pacella E, Pescosolido N, Tranquilli-Leali FM, Feher J. Age-related changes in the human optic nerve. *Can J Ophthalmol*. 2002;37(7):389-394. doi: 10.1016/s0008-4182(02)80040-0
13. Yew DT. Aging in retinas and optic nerves of 2.5- to 9-month-old mice. *Acta Anat (Basel)*. 1979;104(3):332-334. doi: 10.1159/000145079
14. Sing NM, Anderson SF, Townsend JC. The normal optic nerve head. *Optom Vis Sci*. 2000;77(6):293-301. doi: 10.1097/00006324-200006000-00009
15. Trapp BD, Nave KA. Multiple Sclerosis: an immune or neurodegenerative disorder? *Annual Rev Neurosci*. 2008;31:247-269. doi: 10.1146/annurev.neuro.30.051606.094313
16. Ricci A, Bronzetti E, Amenta F. Effect of ageing on the nerve fibre population of rat optic nerve. *Gerontology*. 1988;34(5-6):231-235. doi: 10.1159/000212960
17. Fox JG, Cohen BJ, Loew FM. Laboratory animal medicine. USA Academic Pres. 1984:95.
18. Hirsch FR, Varela-Garcia M, Bunn PA Jr, et al. Epidermal growth factor receptor in non-small-cell lung carcinomas: correlation between gene copy number and protein expression and impact on prognosis. *J Clin Oncol*. 2003;21(20):3798-3807. doi: 10.1200/JCO.2003.11.069
19. Kiyosawa I. Age-related changes in visual function and visual organs of rats. *Exp Anim*. 1996;45(2):103-114. doi: 10.1538/expanim.45.103
20. Sturrock RR. Changes in the number of axons in the human embryonic optic nerve from 8 to 18 weeks gestation. *J Hirnforsch*. 1987;28(6):649-652.
21. Butt AM, Kirvell S. Glial cells in transected optic nerves of immature rats. II. an immunohistochemical study. *J Neurocytol*. 1996;25(6):381-392. doi: 10.1007/BF02284809
22. Attia H, Taha M, Abdellatif A. Effects of aging on the myelination of the optic nerve in rats. *Int J Neurosci*. 2019;129(4):320-324. doi: 10.1080/00207454.2018.1529670
23. Yassa HD. Age-related changes in the optic nerve of Sprague-Dawley rats: an ultrastructural and immunohistochemical study. *Acta Histochem*. 2014;116(6):1085-1095. doi: 10.1016/j.acthis.2014.05.001
24. Lam K, Sefton AJ, Bennett MR. Loss of axons from the optic nerve of the rat during early postnatal development. *Brain Res*. 1982;255(3):487-491. doi: 10.1016/0165-3806(82)90014-1
25. Wong SL, Ip PP, Yew DT. Comparative ultrastructural study of the optic nerves and visual cortices of young (2.5 months) and old (17 months) mice. *Acta Anat (Basel)*. 1979;105(4):426-430. doi: 10.1159/000145149
26. Triviño A, Ramírez JM, Salazar JJ, Ramírez AI, García-Sánchez J. Immunohistochemical study of human optic nerve head astroglia. *Vision Res*. 1996;36(14):2015-2028. doi: 10.1016/0042-6989(95)00317-7
27. Hernandez MR, Igoe F, Neufeld AH. Extracellular matrix of the human optic nerve head. *Am J Ophthalmol*. 1986;102(2):139-148. doi: 10.1016/0002-9394(86)90134-0
28. Hernandez MR, Luo XX, Andrzejewska W, Neufeld AH. Age-related changes in the extracellular matrix of the human optic nerve head. *Am J Ophthalmol*. 1989;107(5):476-484. doi: 10.1016/0002-9394(89)90491-1
29. Cepurna WO, Kayton RJ, Johnson EC, Morrison JC. Age related optic nerve axonal loss in adult Brown Norway rats. *Exp Eye Res*. 2005;80(6):877-884. doi: 10.1016/j.exer.2004.12.021
30. Gabilondo I, Martínez-Lapiscina EH, Martínez-Heras E, et al. Trans-synaptic axonal degeneration in the visual pathway in multiple sclerosis. *Ann Neurol*. 2014;75(1):98-107. doi: 10.1002/ana.24030
31. Tur C, Goodkin O, Altmann DR, et al. Longitudinal evidence for anterograde trans-synaptic degeneration after optic neuritis. *Brain*. 2016;139(3):816-828. doi: 10.1093/brain/awv396
32. Compston A, Coles A. Multiple sclerosis. *Lancet*. 2008;372(9648):1502-1517. doi: 10.1016/S0140-6736(08)61620-7
33. Lucchinetti C, Brück W, Parisi J, Scheithauer B, Rodriguez M, Lassmann H. Heterogeneity of multiple sclerosis lesions: implications for the pathogenesis of demyelination. *Ann Neurol*. 2000;47(6):707-717. doi: 10.1002/1531-8249(200006)47:6<707:aid-ana3>3.0.co;2-q
34. Compston DAS. McAlpine's multiple sclerosis. 4th edn. London: Elsevier, 2005:589.
35. Skoff RP, Toland D, Nast E. Pattern of myelination and distribution of neuroglial cells along the developing optic system of the rat and rabbit. *J Comp Neurol*. 1980;191(2):237-253. doi: 10.1002/cne.901910207